Esterification processes based on functionalized mesoporous solids

Maciej Trejda *, Beata Pokora, Maria Ziolek

Adam Mickiewicz University in Poznań, Faculty of Chemistry, Umultowska 89b, PL-61-614 Poznań, Poland

A B S T R A C T

The abilities of niobium and manganese to enhance oxidation of thiol groups in (3-mercaptopropyl)trimethoxysilane (MPTMS) used for functionalization of SBA-15 and MCF materials, by hydrogen peroxide in order to form catalysts with acidic properties were evaluated. Materials obtained were characterized by: N_2 adsorption, XRD, XRF, elemental and thermal analyses and titration of acid sites. The highest concentration of acidic sites was found for SBA-15 structure modified with niobium. The catalytic activities of materials obtained were examined in esterification of acetic acid with ethanol and 2-propanol. Both niobium containing samples (MP-NbSBA-15 and MP-NbMCF) showed high yields of ethyl and 2-propyl acetate. The amount of 2-propyl acetate formed was found to linearly depend on the number of acid sites on the catalyst surface. The reuse tests proved that the drop in the catalyst activity in consecutive catalytic cycles is not too high, which suggests possible application of the materials obtained after further optimization.

© 2014 Elsevier B.V. All rights reserved.

1. Introduction

Esterification is a very important process in organic synthesis [1] as well as in fuel industry [2] mainly related to biodiesel production (formation of fatty acid esters). Despite the lower cost of fossil fuel in relation to biodiesel, the production of latter fuel is still increasing as this fuel is more environmentally friendly [3]. Esterification processes used in industry are mainly carried out in homogeneous phase in the presence of acidic catalysts like H_2SO_4, HCl, H_3PO_4 or *p*-toluene sulphonic acid. It implies some difficulties related to corrosion of the apparatus, separation of products and wastes. These problems can be overcome by the application of solid catalysts having acidic centres on the surface. Moreover, solid catalysts offer a possibility to conduct reactions in continuous, fixed bed reactors [4].

As mentioned above, esters of fatty acids are used in large quantities for biodiesel production. However, other esters of organic acids have a variety of applications. One of the acids commonly used for esterification is acetic acid. Transformation of this acid with ethanol leads to ethyl acetate, which is an important compound for many applications in chemical industry. For instance, ethyl acetate is used for the production of adhesives, coatings, perfumes or plasticizers [5]. 2-Propyl acetate is obtained in esterification of acetic acid with 2-propanol and mainly used as a solvent. Moreover, the heat

of combustion of ethyl acetate and 2-propyl acetate is ca. 50% and 35% lower, respectively, than for e.g. methyl oleate. This does not exclude the use of both esters as additives for biodiesel and what is more ethyl and 2-propyl acetates increase the cold resistance of biofuel.

Different heterogeneous catalysts were tested in the esterification of acetic acid with ethanol and 2-propanol, including carbon materials [6,7], zeolites [4,5,8], aluminophosphates [9], mesoporous solids [10], heteropolyacids [11–13] also including group five elements [12], montmorillonite [14] or resins [15–17]. However, because of the nature of esterification processes the very high yield of ester is limited by reaction equilibrium. It can be overcome by favouring of the product side by either the use of one reactant in excess over the other or the continuous removal of water formed [1].

In our previous works we developed a method for efficient formation of acid catalysts based on mesoporous materials functionalized with (3-mercaptopropyl)trimethoxysilane (MPTMS) [18,19]. The materials obtained were applied in acetic acid esterification with glycerol. It has been found that in the process mentioned, which proceeds via three steps (formation of monoacetylglycerols, diacetylglycerols and finally triacetylglycerol) not only the number but also the strength of acidic sites determine the formation of the target product, i.e. triacetylglycerol. In that case the catalytic results were not straightly dependent on acid site number. Therefore, in this paper we would like to check these properties in single step process. For that purpose the esterification of acetic acid with ethanol and 2-propanol

---

(i.e. processes that are also relevant for industry) were chosen. Moreover, these processes were not much investigated using catalytic system applied in this study, especially in relation to MCF materials having high pore diameter. In this paper we obtained a series of catalysts differing in the number of acid sites, using the same methodology of preparation. For this purpose niobium and manganese were chosen as modifiers of mesoporous materials. Both metals play an important role in the oxidation of SH groups to sulphonic ones by H_2O_2 as evidenced in [20]. On the other hand manganese easily changes its oxidation state contrary to niobium species and it is more hardly introduced to mesoporous silica structure if used in the form of cationic species and under the conditions applied for SBA-15 and MCF syntheses. One can expect that such differences will be reflected in the anchoring of MPTMS and oxidation of SH groups to SO_3H and moreover, will allow checking if the effectiveness of oxidation of thiol groups by H_2O_2 depends or not on the incorporation of transition metal into the silica structure.

2. Experimental

2.1. Preparation of SBA-15 type catalysts

SBA-15 catalysts functionalized with MPTMS, (3-mercaptopropyl)trimethoxysilane and modified with Nb or Mn were prepared via hydrothermal synthesis. The synthesis was performed in polypropylene bottle (PP). The synthesis procedure was as follows. To the PP bottle the Pluronic P123 (Poly(ethylene glycol)-block–poly(propylene glycol)-block–poly(ethylene glycol)) (Aldrich—8 g), HCl (Chempur 35%—17.52 g) and water (282.5 g) were added. When the surfactant was dissolved a TEOS (Aldrich—17.054 g) was dropwise inserted. After 45 min MPTMS (Aldrich—1.69 g) and hydrogen peroxide (Merck 35%—7.17 g) were added. For metal containing samples, ammonium niobate(V) oxalate (Aldrich) or manganese(II) nitrate tetrahydrate (Aldrich) were also added to the gel (10 min after TEOS addition) keeping Si/Nb or Si/Mn molar ratio 64. Final mixture was stirred at 313 K for 20 h and then heated at 373 K under static conditions for 24 h. The product was washed with water and dried at RT. The template was removed by constant extraction with ethanol in Soxhlet apparatus.

2.2. Preparation of MCF type catalysts

MCF catalysts functionalized with MPTMS, (3-mercaptopropyl)trimethoxysilane and modified with Nb or Mn were prepared via hydrothermal synthesis similar like for SBA-15. 1,3,5-trimethylbnzene (Aldrich—12 g) and NH_4F (Aldrich—0.0934 g) were added under vigorous stirring after dissolving of Pluronic P123. TEOS was added one hour after 1,3,5-trimethylbenzene and NH_4F addition. Next steps were the same as for SBA-15.

2.3. Characterization techniques

The materials prepared were characterized using different analytical techniques: N_2 adsorption/desorption, XRD, XRF, elemental analysis and amperometric titration.

XRD patterns were recorded at room temperature on a Bruker AXS D8 Advance apparatus using Cu $K\alpha$ radiation ($\alpha = 0.154$ nm), with a step of $0.02°$ and $0.05°$ in the small-angle and wide-angle, respectively.

N_2 adsorption/desorption isotherms were obtained on a Micrometrics ASAP 2010. First, samples (200 mg) were outgassed under vacuum at 423 K to remove water or solvent, like ethanol from pores. The surface area was calculated using the BET method. Pore volume, cells and windows diameter of MCF materials were estimated according to Broekhoff-de Boer method with Frenkel–Halsey–Hills approximation [21].

X-ray fluorescence (XRF) using MiniPal-Philips instrument was applied to determine the real molar ratio of Si/Nb or Ta in materials prepared. The calculations were performed using calibration curve based on reference mixtures of silica (Degussa) and metal oxide Nb_2O_5 (Alfa Aesar). The calibration curves consisted of 10 points related to different Si/Nb molar ratio in the range from 3 to 300. The metal concentration in a sample was established by the amount of emitted X-ray radiation related to the values in the calibration curves.

Elemental analyses of materials obtained were performed using Elementar Analyser Vario EL III.

Titration of acidic sites was performed using 100 mg of anhydrous material (dried at 423 K for 12 h). Catalyst was immersed in a 2 M NaCl solution (60 cm³) and stirred at RT for 18 h. After this time the solution was titrated with 0.005 M NaOH solution.

2.4. Esterification processes

Esterification of acetic acid with ethanol or 2-propanol was performed in a liquid phase in batch reactor without usage of any solvents. The reactor was equipped with a condenser and a process was conducted at autogenously pressure. The reaction was carried out for 4 h at 363 K and 373 K for ethanol and 2-propanol, respectively. Before reaction catalyst was activated in oven at 423 K for 12 h. 12 g of acetic acid was used for all reaction keeping molar ratio of acetic acid to alcohol 2:1. The volume of solution after the reaction was checked each time to indicate that there is no leak in the system. For selected catalysts the reuse test was performed. Prior this process the catalyst after the first run of reaction was separated from reactant mixture by centrifugation and dried in oven overnight at 423 K. Then the catalysts were applied for the next use. The composition of products were analysed by a gas chromatograph (Thermo Scientific—Focus) equipped with 60 m DB-1 capillary column, worked at the temperature range of 313–523 K (temperature ramp 10 K min⁻¹), and MS detector. The quantitative analysis were performed by acetic acid titration with sodium hydroxide solution.

3. Results and discussion

3.1. Texture/structure parameters

Two different types of mesoporous materials, i.e. SBA-15 and MCF, were functionalized with MPTMS using one-pot synthesis procedure in the presence of hydrogen peroxide. H_2O_2 was applied to oxidize thiol species. Moreover, the materials were also modified with Mn or Nb mainly to enhance the efficiency of sulphonic species formation [22]. The choice of different structured materials (SBA-15 with hexagonally ordered mesopores and mesoporous cellular foams (MCF) containing big cells and windows) was dictated by the expected differences in the location of the active sites and in their availability to reagents. SBA-15 based samples show typical XRD patterns characteristic of this solid material (Fig. 1). An intensive peak assigned to (1 0 0) plane is observed at 2 theta below 1°. The structure of SBA-15 samples is also ordered in long distance, which is testified by the presence of two additional peaks at 2 theta between 1 and 2º. These peaks are assigned to (1 1 0) and (2 0 0) planes, respectively. XRD patterns of MCF materials do not show peaks in this region (data not shown here). This is typical of samples with relatively high mesoporous diameter. It is known, that the increase in pore diameter shifts the position of (1 0 0) plane to a lower value of 2 theta.

The structure of MCF materials can be confirmed by their sorption properties. Fig. 2 presents the N_2 adsorption/desorption isotherms and the parameters calculated from it are shown in Table 1. The shape of isotherms presented in Fig. 2 is
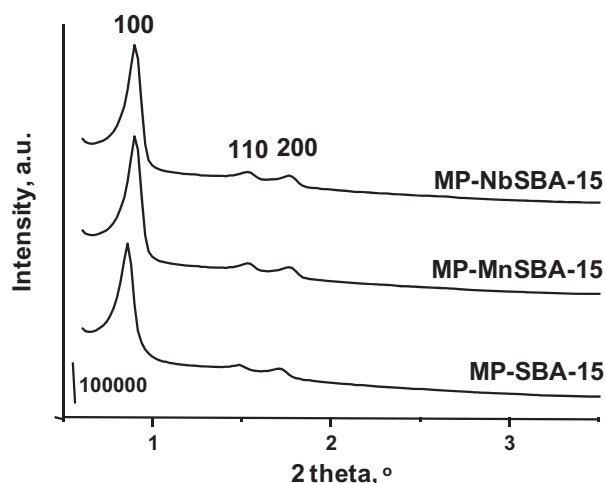
Fig. 1. XRD patterns of SBA-15 materials modified with MPTMS.

characteristic of MCF materials as shown in literature [21,23]. All samples show a hysteresis loop that is caused by difference in p/p_0 between capillary condensation and evaporation. The surface area measured for MCF samples is relatively high, in the range from 580 to 640 m^2 g^{-1}. A larger surface area is observed for SBA-15 materials (710–740 m^2 g^{-1}). Independently of mesoporous structure type the highest surface area and pore volume is observed for Mn containing samples. However, except for sample MP-NbSBA-15, this difference is not very significant. MP-NbSBA-15 material shows a different N$_2$ adsorption/desorption isotherm (Fig. 2). A sharp increase in N$_2$ amount adsorbed is not observed in the range of p/p_0 from 0.5 to 0.8. Moreover, nitrogen desorbs from mesopores at a lower p/p_0 value. It can be explained by some pore blockage that is manifested in lower pore diameter calculated from the desorption branch of the isotherm. In fact, MP-NbSBA-15 contains about two times more niobium species than MP-NbMCF and it is probable that a part of niobium is located within pores in the form of niobium oxide which blocks the pores.

It is important to add a comment about low efficiency of manganese incorporation into both mesoporous structures. It is known that when using nonionic template and high acidic pH, manganese in forms of cations is not sufficiently involved in the formation of gel. A higher efficiency of Mn incorporation can be achieved using a higher pH value and the pre-hydrolyzing approach [24]. However, the presence of Mn salt in the synthesis gel even at very acidic conditions changes evidently the surface properties (mainly the acidity of the surface).

3.2. Incorporation efficiency and state of MPTMS

An important parameter that should be considered as a key factor determining the MPTMS incorporation efficiency is the type of silica structure. Table 2 presents the amount of MPTMS expressed as mmol of sulphur per 1 g of solid. This value is ca. 0.8 and 0.9 mmol g^{-1} for MCF and SBA-15 materials, respectively. A higher efficiency of MPTMS incorporation obtained for SBA-15 samples is in line with previous works [18,19]. Moreover, the efficiency of MPTMS incorporation does not depend on chemical composition of mesoporous solids. Very similar amounts of sulphur are detected on Nb and Mn containing samples as well as on mesoporous silica of the same mesoporous structure (SBA-15 or MCF). Moreover, one can observe that C/S molar ratio for some samples is higher than 5. It means that some carbon present in the sample not origin from MPTMS anchored (organosilane is bonded to the surface at least by one methoxy group). The presence of carbon excess can be explained by residual template not extracted from the material. For example, the amount of carbon in MCF is higher than in MnMCF, 8.3 and 5.9 mmol g^{-1}, respectively. The latter sample has a higher windows diameter, which could be important factor influencing the effectiveness of template removal.

From the catalytic point of view, not only the amount of organosilane incorporated is important but also the efficiency of thiol species oxidation is crucial. To differentiate the amount of sulphonic species, besides the silica materials, two other samples were prepared in the presence of Mn and Nb, respectively. The metal choice was based on literature data showing the ability of Mn and Nb to interact with hydrogen peroxide to form active oxygen species. The latter metal was previously proved to enhance the formation of sulphonic species [22].

The oxidation of SH group from MPTMS takes place during hydrothermal synthesis in the presence of hydrogen peroxide. Therefore, it should be assumed that all metal precursor added to the synthesis mixture takes part in the interaction with the oxidant. However, in the final material the concentration of both metals is different than in the synthesis gel. Whereas niobium is easily incorporated into SBA-15 structure and a little bit worse to MCF one, Mn is hardly introduced into both structures in the conditions applied in this study (Table 2).

The first information concerning the efficiency of thiol species oxidation comes from DTA analyses. The thiol and sulphonic species content on the material surface can be estimated from different decomposition temperatures observed for both species. Whereas thiol species decompose at ca. 600–650 K, the decomposition of sulphonic groups occurs at ca. 800 K [25,26]. Fig. 3 shows DTA curves of SBA-15 and MCF materials functionalized with MPTMS. For both silicas the main exothermic peak is observed at ca. 550–580 K showing the domination of SH species in the samples. Only for MP-SBA-15, the maximum at a higher temperature is slightly visible. For the samples synthesized in the presence of Mn, the exothermic peaks are well visible irrespective of material structure, however the participation of thiol species is still significant. This is not the case for the niobium containing samples. For MP-NbSBA-15, the DTA curve points to the presence of only sulphonic species, whereas for MP-NbMCF some traces of thiol species are detected.
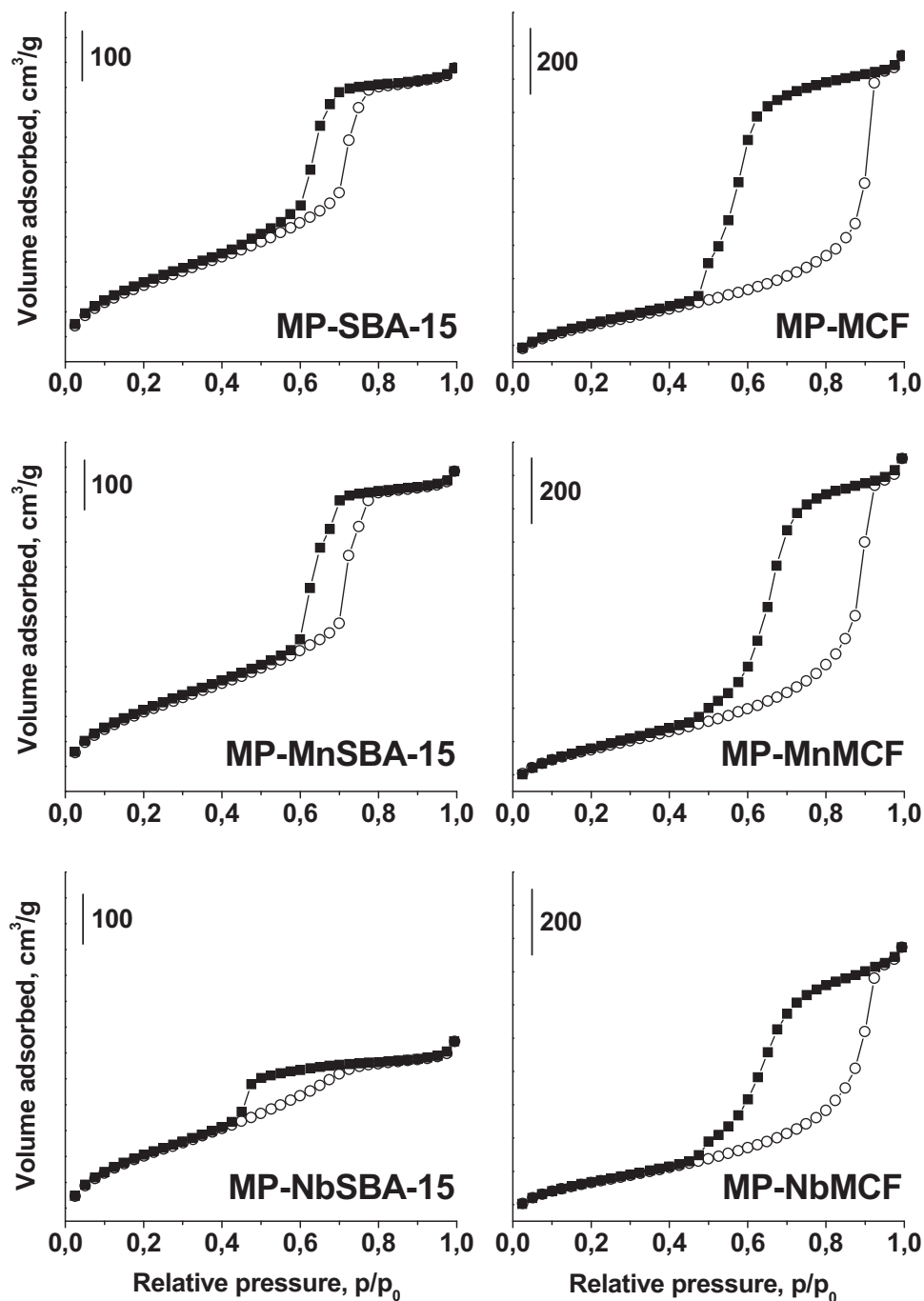
Table 1
Textural/structural characterization.

Catalyst	Surface area (m^2 g^{-1})	Pore volume[a] (cm^3 g^{-1})	Average pore diameter (nm)	
			adsorption	desorption
MP-MCF	590	1.69	27.8[b]	6.1[c]
MP-MnMCF	640	1.81	22.4[b]	7.4[c]
MP-NbMCF	580	1.50	27.9[b]	6.9[c]
MP-SBA-15	730	1.04	6.4	6.9
MP-MnSBA-15	740	1.15	6.4	6.4
MP-NbSBA-15	710	0.65	6.0	4.6

[a] Determined from adsorption branches of N$_2$ isotherms (BdB–FHH method).
[b] Cells diameter as determined from adsorption branches of N$_2$ isotherms (BdB–FHH method).
[c] Windows diameter as determined from desorption branches of N$_2$ isotherms (BdB–FHH method).

Fig. 2. N_2 adsorption/desorption isotherms.

Table 2
Results of elemental analysis, XRF, ICP and titration of acid sites.

Catalyst	Si/M molar ratio[a]		C (mmol g^{-1})	S (mmol g^{-1})	H$^+$ measured by NaOH titration (mmol g^{-1})
	Started	Final			
MP-MCF	–	–	8.3	0.77	0.30
MP-MnMCF	64	∝	5.9	0.77	0.33
MP-NbMCF	64	127	4.0	0.78	0.77
MP-SBA-15	–	–	5.8	0.91	0.58
MP-MnSBA-15	64	∝	4.9	0.87	0.61
MP-NbSBA-15	64	58	3.4	0.89	0.96

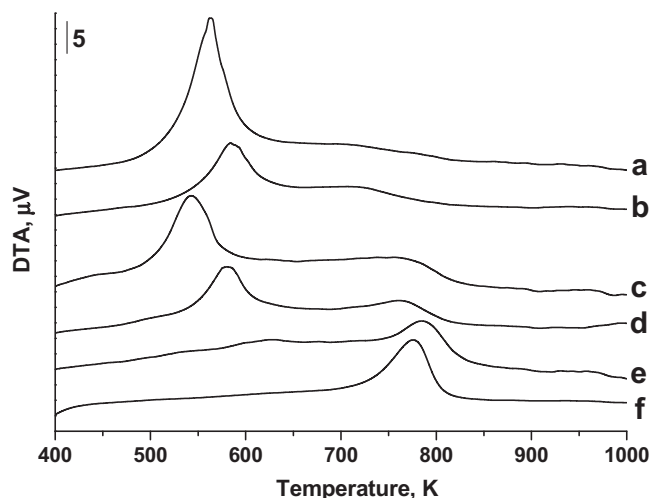[a] Nb estimated by XRF analysis; Mn estimated by ICP.

Fig. 3. DTA profiles of: (a) MP-MCF; (b) MP-SBA-15; (c) MP-MnMCF; (d) MP-MnSBA-15; (e) MP-NbMCF; (f) MP-NbSBA-15.

The concentrations of sulphonic species were determined by acid site titration using sodium hydroxide solution. The results are presented in Table 2. The number of acid centres is higher for the materials of SBA-15 structure than for MCF, irrespectively of the chemical composition of the solid. The addition of Mn to the synthesis gel allows a small increase in the number of acid sites. It suggests that not only formation of peroxo species in the synthesis gel but also the metal location on material surface could have an impact on thiol species oxidation. This is the case of niobium containing samples, which showed a high efficiency of metal incorporation. For MP-NbMCF sample the number of acid sites per gram of the solid measured by titration technique is almost the same as the number of sulphur determined by elemental analysis, whereas for MP-NbSBA-15 it is even higher. It confirms a high efficiency of thiol species oxidation. The higher content of acidic sites calculated from titration in comparison with the amount of sulphur suggests the additional acidity coming from niobium species located outside the walls of SBA-15 material.

3.3. Acetic acid esterification

Esterification of acetic acid with ethanol was performed in the liquid phase using 0.25 g of catalysts prepared in this study as well as in the presence of Nafion SAC 13 applied as a reference material. The application of equimolar amount of reactants lead to the overall yields of ethyl acetate of ca. 67% [5]. Therefore, the acetic acid esterification with alcohols is usually carried out using an excess of one of reagents. More often a higher amount of ethanol is used in the reaction [6,11], however the overload of acetic acid is also applied [9,14]. In our previous works concerning the esterification of acetic acid with glycerol, the excess of the first reactant was used to increase utilization of glycerol [18,19]. Taking into account our earlier works in this paper we applied the molar ratio of acetic acid to ethanol 2.

At the beginning of the study MP-NbMCF material was selected for examination of ethyl acetate formation efficiency depending on the reaction time. This choice was based on the previous work that has shown very high activity of a similar material in acetic acid esterification with glycerol [27]. MP-NbMCF catalyst enhances the reaction rate and the equilibrium of the process is almost obtained after 4 h (Fig. 4). In the next 2 h the formation of ethyl acetate is just by 0.01 mmol higher. The process was also performed without the catalyst. This kind of reaction proceeds rather slow and a long time is needed to reach equilibrium. In the absence of the catalyst the
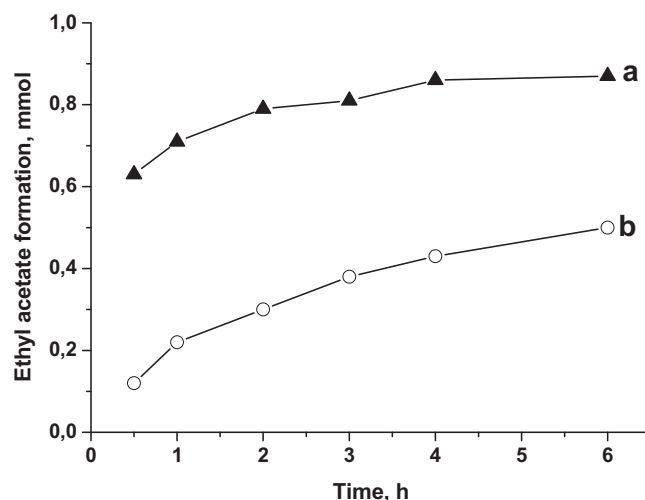

Fig. 4. Ethyl acetate formation vs. reaction time: (a) MP-NbMCF; (b) without catalyst (mass of catalyst—0.25 g; reaction temperature 363 K; acetic acid 0.2 mmol; ethanol 0.1 mmol).
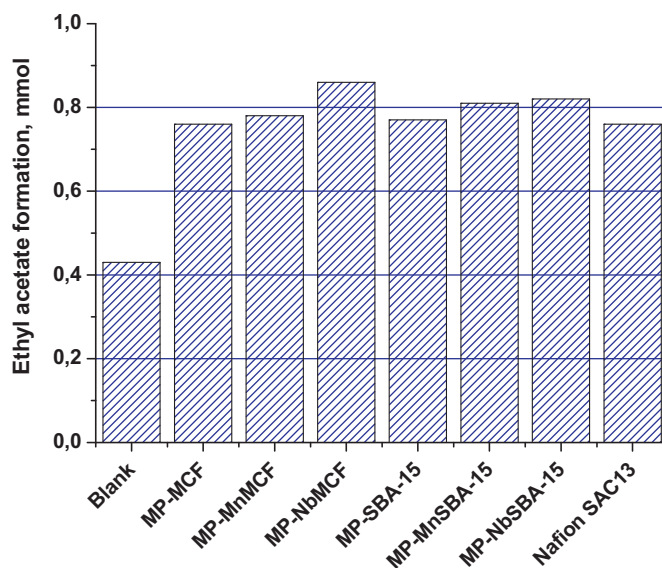

Fig. 5. Ethyl acetate formation on different catalysts (mass of catalyst—0.25 g; reaction temperature 363 K; acetic acid 0.2 mmol; ethanol 0.1 mmol).

formation of ethyl acetate increases almost linearly up to 6 h of the reaction.

On the basis of the above-described results, the optimum reaction time was established as 4 h. The amount of ethyl acetate formation in the presence of all catalysts prepared is presented in Fig. 5. The highest catalytic activity was obtained for MP-NbMCF material (0.86 mmol). This value was by ca. 13% higher than for Nafion SAC 13 used as a reference material. Nafion SAC 13 showed comparable activity to both silicas (SBA-15 and MCF) functionalized with MPTMS. In similar reaction conditions (363 K and acetic acid to ethanol molar ratio of 2:1) but for twice longer reaction time, in the presence of heteropolyacid loaded on montmolillonite K10 the amount of ethyl acetate formed was 0.76 mmol [14], whereas MgAlPO$_4$ (reaction temperature 473 K and acetic acid to ethanol molar ratio = 2:1) was even less active leading to ca. 0.60 mmol of acetic acid [14].

For the sake of comparison, the same reaction time (4 h) was applied for the acetic acid esterification with 2-propanol. The results obtained are presented in Fig. 6. The amount of 2-propyl
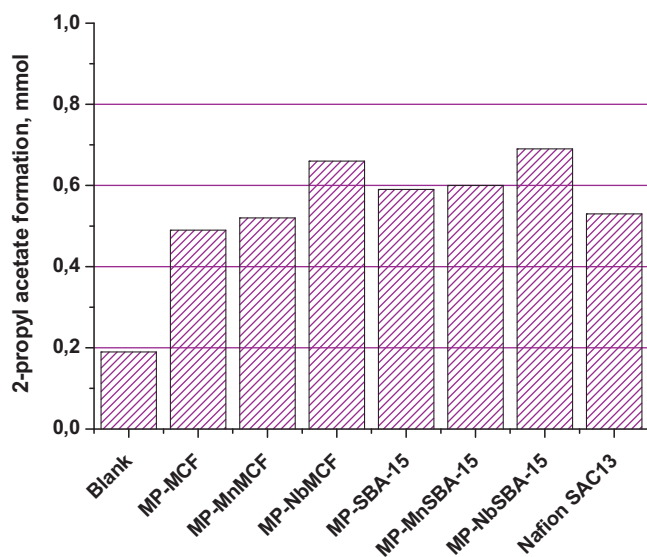
Fig. 6. 2-Propyl acetate formation on different catalysts (mass of catalyst—0.25 g; reaction temperature 373 K; acetic acid 0.2 mmol; 2-propanol 0.1 mmol).
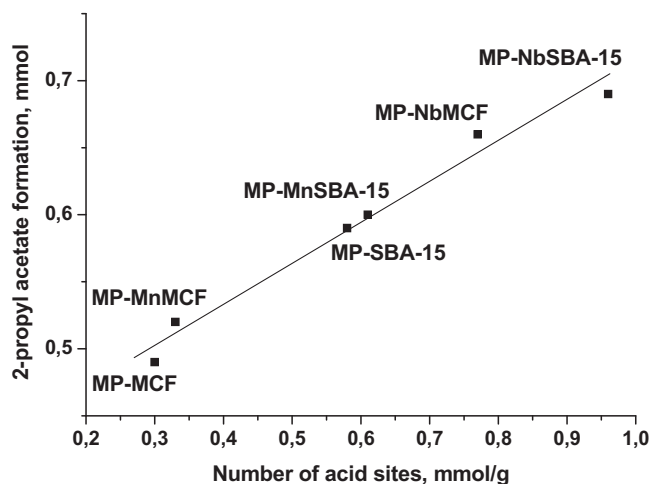

Fig. 8. Reuse test of MP-NbSBA-25 and MP-NbMCF in acetic acid esterification with 2-propanol (mass of catalyst—0.25 g; reaction temperature 373 K; acetic acid 0.2 mmol; 2-propanol 0.1 mmol).

Fig. 7. 2-Propyl acetate formation vs. number of acid sites (mass of catalyst—0.25 g; reaction temperature 373 K; acetic acid 0.2 mmol; 2-propanol 0.1 mmol).

acetate formed (mmol) is lower than that obtained in the reaction involving ethanol (Fig. 5). This is in line with literature showing that esterification proceeds slower when an alcohol with a longer carbon chain is used in the reaction [16]. The most active material (MP-NbSBA-15) leads to obtaining 0.69 mmol of 2-propyl acetate. This value is by 30% higher than for Nafion SAC 13 (0.53 mmol). The yields of 2-propyl acetate obtained in this work are much better than those obtained for polymer-supported fibre catalyst (Smopex-101) [16], however the latter process was conducted at a different temperature of 333 K and acetic acid to 2-propanol ratio of 1:1.

The difference in activity of the catalysts is higher for the reaction involving 2-propanol (Fig. 6) than ethanol (Fig. 5). It can be explain by the fact that esterification of acetic acid with 2-propanol does not reach equilibrium after 4 h and the number of acidic sites has a higher impact on the results obtained. Fig. 7 shows the relationship between the amount of 2-propyl acetate formed and the number of acidic sites on the catalyst surface. Indeed, a linear dependence can be observed and no impact of the material structure is noticed. This trend is not seen for ethanol after 4 h of reaction, because as it was above-mentioned, the reaction is close to equilibrium. From the point of view of industrial applications, an
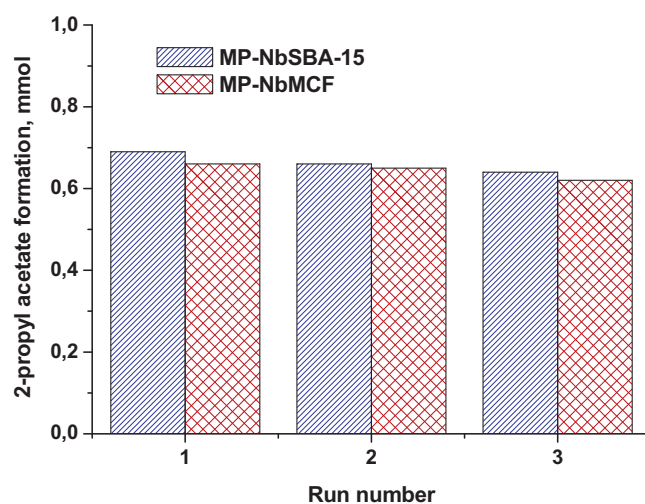
important factor is the catalyst ability to be stable in as many as possible subsequent catalytic cycles. Even similar materials can differ in this matter. For example carbon based materials were examined in acetic acid esterification with ethanol [6,7]. While the materials obtained from polycyclic aromatic carbon sheets with attached SO_3H groups showed very stable activity in acetic acid esterification with ethanol [6], the materials based on carbon nanotubes and carbon xerogels showed poor stability in this process [7]. MCF and SBA-15 type materials functionalized with MPTMS were previously found to be stable in acetic acid esterification with glycerol [18,19]. The stabilities of most active catalysts obtained in this study were tested in acetic acid esterification with 2-propanol and the results are presented in Fig. 8. Both niobium containing materials show a little decrease in ester formation, 0.05 and 0.04 mmol drop for MP-NbSBA-15 and MP-NbMCF, respectively. These values of the activity drop are not too high and it is expected that the materials will be attractive for possible applications after further optimization.

4. Conclusions

The reported results allow us to draw conclusions regarding materials chemistry and catalysis. It has been documented that the nature of transition metal (Nb or Mn) present in the synthesis gel does not play important role in the effectiveness of MPTMS anchoring, whereas the structure of mesoporous silica seems to be crucial in this matter (higher amounts of MPTMS anchoring on SBA-15). The important finding is that it is not sufficient to use transition metal which forms peroxo species with H_2O_2 in the reaction mixture during the synthesis of SBA-15 or MCF to oxidise effectively SH groups anchored in mesoporous silica. More important seems to be incorporation of metal to silica walls and its influence on SH oxidation towards SO_3H.

Niobium containing materials revealed higher activity in the production of both, ethyl and 2-propyl acetates than commercial Nafion SAC13 material in the esterification of acetic acid with respective alcohols. The linear correlation between the number of BAS and the 2-propyl acetate production was documented, which was not observed in the acetic acid esterification with glycerol published elsewhere [18,19].

Acknowledgement

References

[1] O. Junzo, Angew. Chem. Int. Ed. 40 (2001) 2044–2045.
[2] M.E. Borges, L. Díaz, Renewable Sustainable Energy Rev. 16 (2012) 2839–2849.
[3] E. Olivetti, E. Gülşen, J. Malça, É. Castanheira, F. Freire, L. Dias, R. Kirchain, Environ. Sci. Technol. 48 (2014) 7642–7650.
[4] J. Bedard, H. Chiang, A. Bhan, J. Catal. 290 (2012) 210–219.
[5] K.-C. Wu, Y.-W. Chen, Appl. Catal., A: Gen. 257 (2004) 33–42.
[6] M. Hara, T. Yoshida, A. Takagaki, T. Takata, J.N. Kondo, S. Hayashi, K. Domen, Angew. Chem. Int. Ed. 43 (2004) 2955–2958.
[7] R.P. Rocha, M.F.R. Pereira, J.L. Figueiredo, Catal. Today 218–219 (2013) 51–56.
[8] S.R. Kirumakki, N. Nagaraju, K.V.R. Chary, Appl. Catal., A: Gen. 299 (2006) 185–192.
[9] M.R. Devi, C. Kannan, J. Environ. Nanotechnol. 2 (2013) 25–28.
[10] K. Nakajima, I. Tomita, M. Hara, S. Hayashi, K. Domen, J.N. Kondo, Adv. Mater. 17 (2005) 1839–1842.
[11] T.V. Kovalchuk, J.N. Kochkin, H. Sfihi, V.N. Zaitsev, J. Fraissard, J. Catal. 263 (2009) 247–257.
[12] D. Park, S. Park, J. Choi, I. Song, Catal. Lett. 135 (2010) 269–274.
[13] H.-K. Min, M.B. Park, S.B. Hong, J. Catal. 271 (2010) 186–194.
[14] H. Gurav, V.V. Bokade, J. Nat. Gas Chem. 19 (2010) 161–164.
[15] S.Q. Merchant, K.A. Almohammad, A.A.M. Al Bassam, S.H. Ali, Fuel 111 (2013) 140–147.
[16] J. Lilja, D.Y. Murzin, T. Salmi, J. Aumo, P. Mäki-Arvela, M. Sundell, J. Mol. Catal. A: Chem. 182–183 (2002) 555–563.
[17] S.H. Ali, S.Q. Merchant, Int. J. Chem. Kinet. 38 (2006) 593–612.
[18] M. Trejda, K. Stawicka, M. Ziolek, Appl. Catal., B—Environ. 103 (2011) 404–412.
[19] K. Stawicka, M. Trejda, M. Ziolek, Appl. Catal., A—Gen. 467 (2013) 325–334.
[20] K. Stawicka, Modified Silicas, Metalosilicates and Metal Oxides – Preparation, Characterization and Application in Esterification with the Participation of Glycerol, Faculty of Chemistry, Adam Mickiewicz University in Poznań, Poznań, 2014 (PhD thesis).
[21] P. Schmidt-Winkel, W.W. Lukens Jr., P. Yang, D.I. Margolese, J.S. Lettow, J.Y. Ying, G.D. Stucky, Chem. Mater. 12 (2000) 686–696.
[22] M. Trejda, K. Stawicka, M. Ziolek, Catal. Today 192 (2012) 130–135.
[23] J.S. Lettow, Y.J. Han, P. Schmidt-Winkel, P. Yang, D. Zhao, G.D. Stucky, J.Y. Ying, Langmuir 16 (2000) 8291–8295.
[24] G. Satish Kumar, M. Palanichamy, M. Hartmann, V. Murugesan, Catal. Commun. 8 (2007) 493–497.
[25] D. Margolese, J.A. Melero, S.C. Christiansen, B.F. Chmelka, G.D. Stucky, Chem. Mater. 12 (2000) 2448–2459.
[26] I. Díaz, C. Márquez-Alvarez, F. Mohino, J.n. Pérez-Pariente, E. Sastre, J. Catal. 193 (2000) 283–294.
[27] M. Trejda, K. Stawicka, A. Dubinska, M. Ziolek, Catal. Today 187 (2012) 129–134.